Vol. 513: 29–37, 2014
doi: 10.3354/meps10954

MARINE ECOLOGY PROGRESS SERIES
Mar Ecol Prog Ser

Published October 22

Vertical distribution of transparent exopolymer particle (TEP) concentration in the oligotrophic western tropical North Pacific

Taketoshi Kodama[1,5,*], Hiroaki Kurogi[2], Makoto Okazaki[1], Tadao Jinbo[3], Seinen Chow[1], Tsutomu Tomoda[4], Tadafumi Ichikawa[1], Tomowo Watanabe[1]

[1]National Research Institute of Fisheries Science, Fisheries Research Agency, 2-12-4, Fukuura, Kanazawa, Yokohama, Kanagawa 236-8648, Japan

[2]Yokosuka Marine Biological Station, National Research Institute of Aquaculture, Fisheries Research Agency, 6-31-1, Nagai, Yokosuka, Kanagawa 238-0316, Japan

[3]Shibushi Marine Biological Station, National Research Institute of Aquaculture, Fisheries Research Agency, 205, Natsui, Shibushi, Shibushi, Kagoshima 899-7101, Japan

[4]Minami-Izu Marine Biological Station, National Research Institute of Aquaculture, Fisheries Research Agency, 183-2, Irouzaki, Minami-Izu, Kamo, Shizuoka 415-0156, Japan

[5]*Present address:* Japan Sea National Fisheries Research Institute, Fisheries Research Agency, 1-5939-22, Suido-Cho, Chuo, Niigata, Niigata 951-8121, Japan

ABSTRACT: Seawater samples were collected during May–June 2013 from 32 stations west of Guam (10° 30′ N–16° N, 140° 30′ E–144° E) at depths of 5–300 m to describe the vertical profile of transparent exopolymer particle (TEP) concentrations. TEP concentration varied from 18 to 69 µg gum xanthan equivalents per liter, which was a similar level to those observed in other open ocean areas, and the vertical profile of the TEP concentration had a subsurface maximum and minimum which was not associated with phytoplankton abundance. The TEP subsurface maximum occurred from the bottom of the mixed layer to the top of the subsurface chlorophyll maximum (SCM) where dissolved oxygen was supersaturated, indicating that the TEP maximum is produced based on active photosynthesis. The TEP subsurface minimum occurred from the bottom of the SCM to 200 m depth, and was characterized by negative preformed-nitrate water which is produced by decomposition of carbon-rich and nitrogen-poor dissolved organic matter. Additionally, water turbulence, which promotes abiotic TEP production, hardly occurred in the TEP subsurface minimum layer because stratification in this layer was most developed in the vertical profiles. Therefore, our results suggest that the low abiotic TEP production may have induced the TEP minimum. Hence, the TEP concentration in the oligotrophic ocean varied both with phytoplankton activities and also abiotic processes.

KEY WORDS: Particulate organic matter · Marine snow · Nutrients · Mariana · Japanese eel

INTRODUCTION

Transparent exopolymer particles (TEPs) are negatively charged polysaccharides which can be visualized by alcian blue staining (Alldredge et al. 1993). Since TEPs are gelatinous and sticky, they act as an adhesive for particles and promote the formation of larger aggregates of organic matter such as marine snow (Passow 2002b). In general, TEP concentration has been shown to have a relationship to phytoplankton abundance, having a positive relationship with chlorophyll *a* (chl *a*) concentration on a global scale

*Corresponding author: takekodama@affrc.go.jp

(Passow 2002b). Therefore, phytoplankton has been suggested as the primary source for TEPs, and TEP concentration is high in the surface productive layer of oceans (Passow et al. 1994, Passow 2002b). TEP is also formed from the coagulation of dissolved organic matter (DOM) which contains colloidal organic matter (Passow & Alldredge 1994, Passow 2000). Coagulation occurs by abiotic processes; Brownian motion, laminar shear and water turbulence are efficient processes to induce the production of TEP from DOM (Passow 2000, Burd & Jackson 2009).

TEPs are thought to be utilized and consumed by bacteria, zooplankton, micronekton and nekton while the TEPs are sinking, during which the TEPs form large biogenic particle flocs (Passow 2002b). For example, stable isotope analysis indicates that leptocephalus larvae of the Japanese eel *Anguilla japonica* may feed on and be able to assimilate marine snow (Miller et al. 2013).

Several studies on vertical profiles of TEP concentration in seawater have been reported from oligotrophic areas: the eastern North Pacific near Hawaii Island (Wurl et al. 2011), the Gulf of Aqaba (Bar-Zeev et al. 2009) and the Mediterranean Sea (Ortega-Retuerta et al. 2010, Bar-Zeev et al. 2011). Vertical profiles of TEP concentration differ among these reports, but one common characteristic is that TEP concentration is not associated with the subsurface chlorophyll maximum (SCM) (Bar-Zeev et al. 2009, 2011, Ortega-Retuerta et al. 2010, Wurl et al. 2011). TEP concentrations have a subsurface maximum just below the surface mixed layer which is not associated with the SCM near Hawaii (Wurl et al. 2011). Ortega-Retuerta et al. (2010) reported that the TEP concentration was highest in the surface mixed layer and decreased with depths to 200 m, and Bar-Zeev et al. (2011) reported that the TEP concentration had a subsurface minimum around the SCM, and the concentration was slightly higher at 300 and 1000 m depths than the SCM in the Mediterranean Sea. Bar-Zeev et al. (2009) reported that TEP concentrations are the same levels near the surface and at the SCM.

These vertical profiles of TEP in oligotrophic oceans indicate that the standing stock phytoplankton abundance possibly is not appropriate as an indicator of the TEP concentration in the oligotrophic ocean areas. However, reports on TEP concentration in the oligotrophic open oceans are insufficient, and the relationship of TEP origin with phytoplankton for oligotrophic waters needs further clarification. In addition, there is no report on TEP concentration in the oligotrophic western North Pacific, where the physical characteristics and primary productivity are different from the eastern North Pacific near Hawaii (Longhurst 2006). Therefore, we aim to describe the vertical profile of TEP concentration and factors affecting the unique vertical profile of the TEP concentration in the oligotrophic western North Pacific.

MATERIALS AND METHODS

Seawater samples were collected in the surface and mesopelagic layers of the oligotrophic western North Pacific (between 10° 30′ N and 16° N and between 140° 30′ E and 144° E) during an R/V 'Kaiyo-maru' cruise from May 23 to June 18, 2013 (KY1302; Fig. 1). Our investigated area and season correspond to those during which the Japanese eel spawns (Chow et al. 2009, Kurogi et al. 2011, Tsukamoto et al. 2011). Water temperature, salinity, dissolved oxygen (DO) and *in vivo* chlorophyll fluorescence data were collected using a CTD sensor (SBE 9plus, Seabird). The water samples for salinity, DO, TEP,

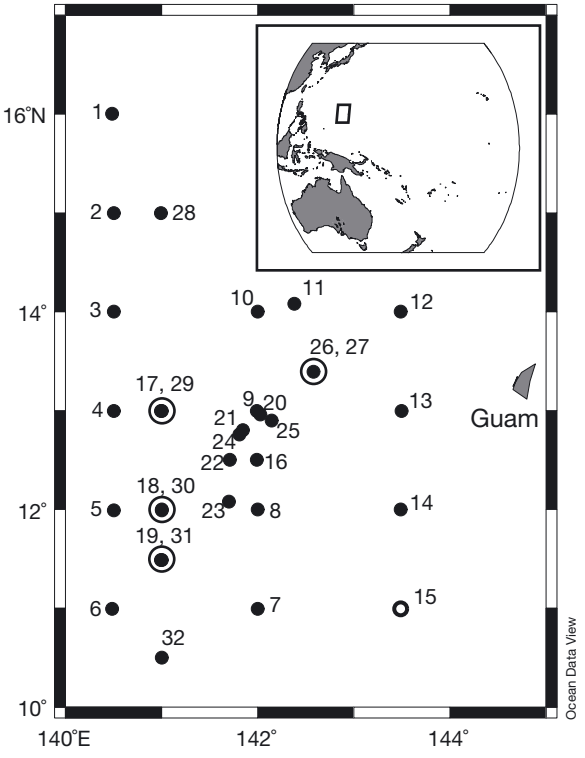

Fig. 1. Sampling stations in the oligotrophic western North Pacific during the R/V 'Kaiyo-maru' cruise. Circles and numbers denote sampling stations and station numbers, respectively. (●) Normal sampling stations; (◉) stations that were observed twice on different days. Stn 15 (O) was not used in the calculation of the water-integrated transparent exopolymer particle (TEP) amount because the TEP concentration in the surface mixed layer was not collected. Inset: location of the sampling area in the Pacific

nutrients and chl *a* concentrations were collected by Niskin bottles mounted on the CTD Rosette Multi-bottle Samplers at 32 stations. The discrete salinity and DO samples were measured by an Autosal (8400B, Guildline Instruments) and a Winkler titration system (Titrinoplus 844, Metrohm), respectively, and used for the calibrations of salinity and DO concentration obtained by the CTD sensor. The mixed layer depth (MLD) was based on a 0.125 unit potential density criterion (Levitus 1982). The Brunt-Väisälä frequency was calculated from the gravitational acceleration (9.80 m s^{-1}), density and the vertical gradient of density (Wunsch & Ferrari 2004).

Water samples (300 ml) for TEP measurement collected from 12 depths (5–300 m) were gently filtered (<150 mmHg) on 0.4 µm pore size Nuclepore membrane filters (47 mm diameter, Whatman), which were stained by 1 ml of alcian blue solution (Passow & Alldredge 1995). After rinsing the alcian blue with 3 ml of Milli-Q water, the filters were stored below −20°C until measurement on land. At each depth, only one sample was collected. The TEP colored by alcian blue was soluble in 6 ml of 80% (14.4 M) sulfuric acid aqueous solution and mixed in the on-land laboratory. After storage for 2 h, the absorbance at 787 nm of the extracted solution was measured by a spectrophotometer (UV-1600, Shimadzu). Absorbance was converted to the weight of gum xanthan equivalent (Xeq) using the calibration curve prepared as follows based on Passow & Alldredge (1995): 21.7 mg l^{-1} and 4.50 mg l^{-1} of gum xanthan aqueous solution were prepared for the standard, and 0.2–2 ml of the standards were filtered onto the membrane filter (each n = 3). These amounts of standards could be filtered smoothly. The recovery factor of gum xanthan was >95% based on the calculation from the increase of the weight of the pre-weighed filters after filtration, which was prepared as a check. Samples of 300 ml filtered Milli-Q water and stain of alcian blue (1 ml) were used as the blank (n = 3). The calibration curve was linear ($r^2 > 0.99$). The minimum detection limit of 7 µg Xeq l^{-1} was estimated to be 3 times the standard deviation of the measurement blanks.

Ten ml of collected seawater for determination of nutrient concentrations (nitrate, nitrite, phosphate and silicate) were collected from 5–300 m depths and stored below −20°C until on-land laboratory analysis. Nutrient concentrations were measured by using a flow injection analyzer (TrAAcs 2000, Bran+Luebbe) at least twice; onece <24 h after thawing and again 36–72 h after thawing. The methods for nitrate + nitrite, nitrite, silicate and phosphate determinations were based on the manual by Hydes et al. (2010). Detection limits were 0.05 µM for nitrite and phosphate, 0.1 µM for nitrate and 0.3 µM for silicate.

For measuring chl *a* concentration in seawater, samples were collected from 5–200 m depths (10 layers). The particles in 300 ml of seawater were collected on a glass fiber filter (GF/F, Whatman), immersed in *N*,*N*-dimethylformamide (Suzuki & Ishimaru 1990) and stored below −20°C in the dark until on-land measurement. Chl *a* concentration was measured by a fluorometer (10-AU, Turner Designs; Welschmeyer 1994). The *in vivo* chlorophyll fluorescence obtained by the fluorometer with CTD was calibrated from the discrete chl *a* concentration for each station. For each station, a linear correlation of the calibration curve was always obtained ($r^2 > 0.87$).

RESULTS

Environmental conditions

The physical structure was uniform in the investigated area, and strong stratification was noted in the surface layer. Temperature in the surface mixed layer was higher than 29°C, and the MLD was 36 ± 12 m (mean ± SD) depth (Fig. 2a). Maximum Brunt–Väisälä frequency was observed at the bottom of the mixed layer and from 150–200 m depth (Fig. 2b).

The chemical and chl *a* distributions were also uniform. The DO concentration had a subsurface maximum at a depth from 50 to 125 m and was supersaturated from the bottom of the surface mixed layer to 100 m depth (Fig. 2c). DO concentration at the subsurface maximum was 211 ± 1.9 µM (n = 32). The DO concentration decreased with depth below 100 m depth (Fig. 2c). Chl *a* concentration was >0.2 µg l^{-1} between 125 and 175 m depth, and the SCM was observed at each station (Fig. 2d). The concentration of chl *a* in the SCM was >0.2 µg l^{-1} (0.27 ± 0.03 µg l^{-1}, n = 32), while the surface chl *a* concentration was 0.05 ± 0.01 µg l^{-1} (at a depth of 5 m, n = 32; Fig. 2d). Nitrate + nitrite was generally depleted from 5 to 125 m depth (e.g. nitrate + nitrite concentration at 125 m was 0.01 ± 0.02 µM [n = 32]), and the concentration was detectable deeper than 150 m (0.17 ± 0.21 µM [n = 32] and 1.20 ± 0.72 µM [n = 31] at 150 and 175 m depths, respectively; Fig. 2e). Phosphate and silicate concentrations were higher than 0.05 µM and 1 µM, respectively, in the nitrate-depleted surface waters. The concentration ratio of nitrate + nitrite to phosphate was <16, and the ratio of nitrate + nitrite to silicate was <1 from 5 to 150 m depths.

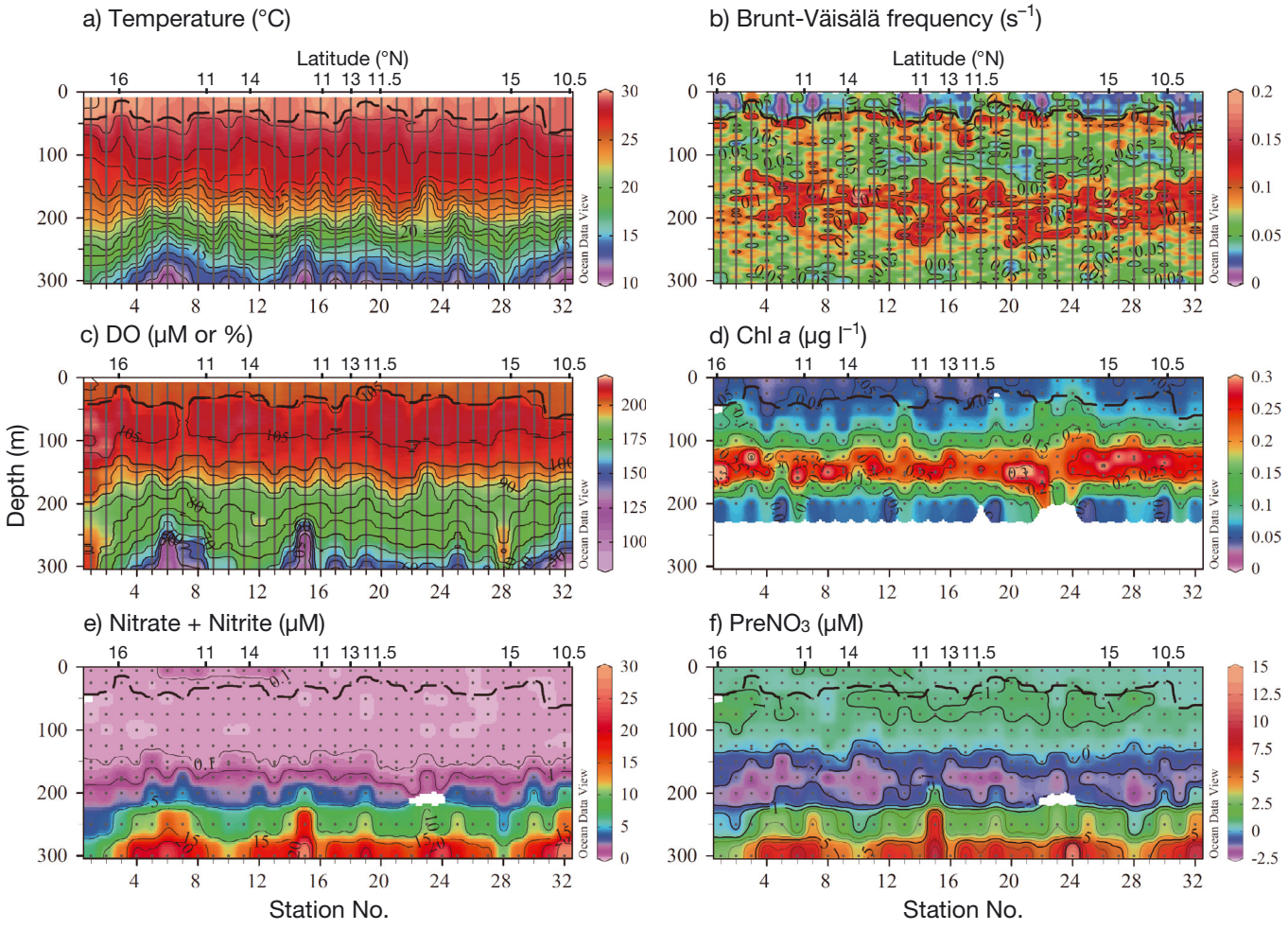

Fig. 2. Vertical profiles of (a) temperature, (b) Brunt–Väisälä frequencies, (c) dissolved oxygen (DO), (d) chl *a*, (e) nitrate + nitrite and (f) preformed nitrate ($PreNO_3$) concentration at the sampling stations. The counters were drawn in Ocean Data View software. Dashed line in every panel denotes mixed layer depth (MLD). Color bar and isoconcentration lines in (c) denote concentration (μM) and saturation (%), respectively

Preformed nitrate ($PreNO_3$) was calculated from the following equation (Johnson et al. 2010):

$$PreNO_3 = NO_3^- - \frac{O_{2Anom}}{R_{O2/NO3}} \quad (1)$$

where O_{2Anom} and $R_{O2/NO3}$ are the difference from DO concentration to DO saturation concentration and the Redfield ratio of oxygen to nitrogen (10.5; Johnson et al. 2010), respectively. $PreNO_3$ had a subsurface maximum at 50 to 75 m depth (0.96 ± 0.28 μM and 1.0 ± 0.18 μM at 50 and 75 m, respectively, n = 32), and was negative and had a minimum at 150 to 200 m at each station (e.g. −0.69 ± 0.5 μM at 150 m, n = 31; Fig. 2f).

From the MLD, DO, calibrated chl *a* fluorescence and $PreNO_3$, the waters could be vertically divided into 5 layers (Fig. 3): surface mixed layer, the oxygen supersaturated (OSS) layer (from the bottom of MLD to the depth at which chl *a* concentration was <0.2 μg l^{-1}), the SCM layer where the chl *a* concentration was >0.2 μg l^{-1}, the negative $PreNO_3$ layer, and the twilight layer where the $PreNO_3$ was positive. The boundaries, except between the surface mixed and the OSS layers, were determined from linear interpolation of the $PreNO_3$ and chl *a* concentrations. Chl *a* concentration was highest in the SCM layer and second highest in the negative $PreNO_3$ and the OSS layers (Table 1). The subsurface maximum of $PreNO_3$ concentration was included in the OSS layer, and it was negative not only in the negative $PreNO_3$ layer but also the SCM layer (Table 1). The highest mean Brunt–Väisälä frequency was observed in the negative $PreNO_3$ layer (Table 1).

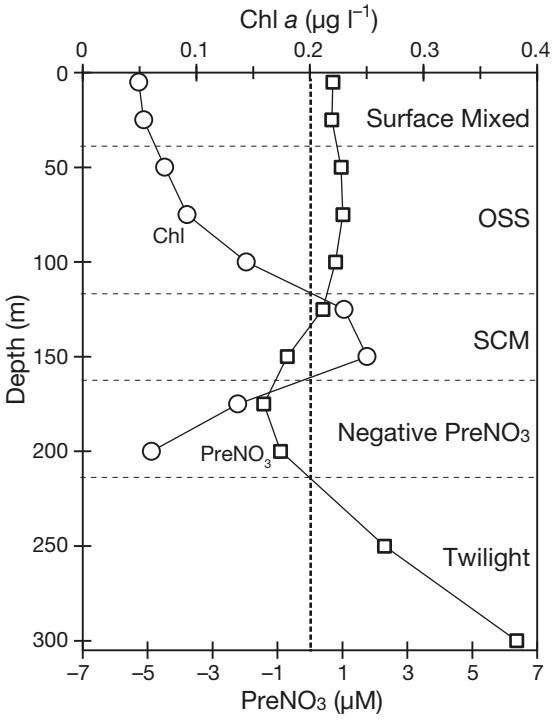

Fig. 3. Vertical profiles over the 5 layers: surface mixed, oxygen supersaturated (OSS), subsurface chlorophyll maximum (SCM), negative preformed-nitrate ($PreNO_3$) and twilight layers. Chl *a* (○) and $PreNO_3$ (□) values are the mean of all stations. Horizontal dashed lines and vertical dotted line indicate the boundaries between the layers and the boundary values of chl *a* concentration (0.2 µg l^{-1}) and $PreNO_3$ concentration (0 µM), respectively

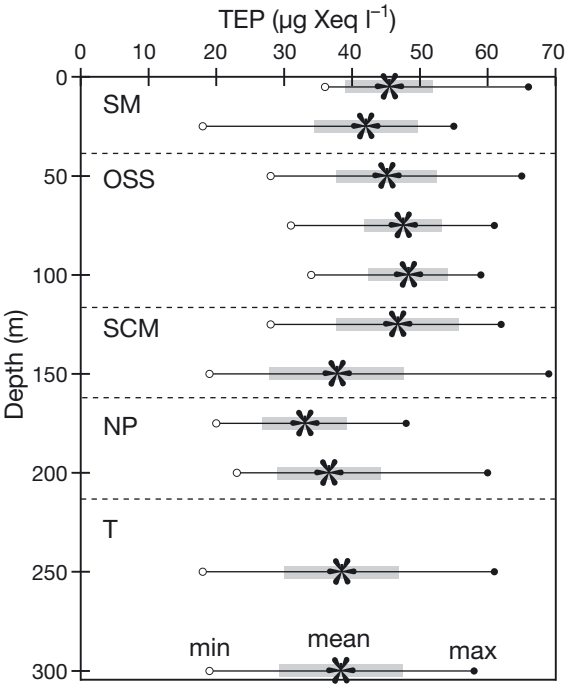

Fig. 4. Vertical profiles of mean transparent exopolymer particle (TEP) concentration from all stations. Mean (✻), minimum (○), maximum (●) concentrations and SD ( ) of each depth are marked. Horizontal dashed lines indicate the boundaries of the layers (same as Fig. 3). Xeq: gum xanthan equivalent, SM: surface mixed, OSS: oxygen supersaturated, SCM: subsurface chlorophyll maximum, NP: negative preformed-nitrate ($PreNO_3$), T: twilight

Variations in vertical concentration of TEP

TEP concentrations varied between 18 and 69 µg Xeq l^{-1} (41.8 ± 9.1 µg Xeq l^{-1}, n = 378) in the investigated area (Fig. 4). The water column-integrated TEP amount from 5 to 300 m depth was 11.1 ± 0.9 g Xeq m^{-2} (n = 31).

The vertical profile of the TEP concentration had a subsurface maximum from 50 to 125 m and a subsurface minimum from 150 to 200 m depth (Fig. 4). Mean TEP concentration in each layer (Table 1) was highest in the OSS layer (47.2 ± 6.4 µg Xeq l^{-1}, n = 99). The second and third highest concentrations were obtained in the surface mixed layer (43.3 ± 7.4 µg

Table 1. Mean ± SD of depth, transparent exopolymer particle (TEP) concentration, chl *a* concentration, preformed nitrate ($PreNO_3$), Brunt–Väisälä frequencies, and TEP:chl *a* ratio in each layer. Different superscripted letters depict significant difference between the layers (1-way ANOVA, $p < 0.05$). n: number of TEP samples, OSS: oxygen supersaturated, SCM: subsurface chlorophyll maximum, Twilight: positive PreNO3 , Xeq: gum xanthan equivalent

Layer	Depth (m)	TEP (µg Xeq l^{-1})	n	Chl *a* (µg l^{-1})	$PreNO_3$ (µM)	Brunt–Väisälä (s^{-1})	TEP:chl *a* (g Xeq g^{-1})
Surface mixed	16 ± 12	43.3 ± 7.4^{a}	61	0.053 ± 0.012^{a}	0.67 ± 0.18^{a}	0.031 ± 0.031^{a}	832 ± 314^{a}
OSS	70 ± 21	47.2 ± 6.4^{b}	99	0.105 ± 0.042^{b}	0.90 ± 0.25^{a}	0.064 ± 0.042^{b}	496 ± 228^{b}
SCM	140 ± 21	42.2 ± 9.8^{a}	89	0.258 ± 0.037^{c}	−0.29 ± 0.59^{b}	0.078 ± 0.050^{c}	169 ± 45^{c}
Negative $PreNO_3$	188 ± 16	35.3 ± 7.1^{c}	63	0.104 ± 0.050^{b}	−1.31 ± 0.45^{c}	0.088 ± 0.052^{d}	402 ± 224^{d}
Twilight	271 ± 30	38.1 ± 9.0^{d}	66	0.053 ± 0.011^{a,*}	4.17 ± 2.72^{d}	0.067 ± 0.036^{b}	806 ± 354^{a}

*Concentration was estimated from *in vivo* chlorophyll fluorescence

Xeq l^{-1}, n = 61) and in the SCM layer (42.2 ± 9.8 µg Xeq l^{-1}, n = 89). The second lowest was in the twilight layer (38.1 ± 9.0 µg Xeq l^{-1}, n = 67) and the lowest was in the negative $PreNO_3$ layer (35.3 ± 7.1 µg Xeq l^{-1}, n = 63). TEP concentration was not significantly different between the surface mixed layer and the SCM layer, but it was significantly different among the other layers (1-way ANOVA, $p < 0.05$; Table 1). The relationship of TEP concentration among the layers was the same when the boundaries of the SCM layer was set as 0.15 µg l^{-1} for the chl *a* concentration.

TEP concentration had a weak but significant positive relationship to DO concentration in all samples ($r = 0.27$, $p < 0.01$, n = 378). However, there was no significant relationship with the chl *a* concentration from 5 to 200 m (n = 317) and chlorophyll fluorescence from 5 to 300 m depth (n = 378). The TEP:chl *a* concentration ratio was not stable among the layers (Table 1); the highest value (832 ± 314 at the surface mixed layer) was approximately 5 times higher than the lowest value (169 ± 45 at the SCM layer). TEP concentration had a weak but significant positive relationship with $PreNO_3$ in the samples collected from the negative $PreNO_3$ and the twilight layers ($r = 0.23$, $p < 0.01$, n = 128). In addition, the minimum of depth-mean TEP concentration at 175 m depth (Fig. 4) was associated with the minimum of the depth-mean $PreNO_3$ concentration (Fig. 3).

DISCUSSION

Comparison of TEP concentration with surveys in other oceans

Samples (300 ml) for the TEP concentration in the present study were collected singly at each depth of each station. Passow (2002b), however, recommends that 3–4 replicate samples are needed for accurate determination of TEP concentration due to the chemical properties of TEP leading to coagulation. Thus, for each station and each depth, the lack of replicate data precludes detailed analyses, and the horizontal variations of TEP concentration could not be evaluated. However, the physical and chemical conditions in our study area were largely homogeneous (Fig. 2), and the sampling stations were concentrated in a narrow area (Fig. 1). Therefore, the mean TEP concentrations for both individual layers (Table 1) and the ocean area (Table 2) can be considered as repre-

Table 2. Comparison of transparent exopolymer particle (TEP) and chl *a* concentrations among the oceans. Values are mean ± SD or range. MLD: mixed layer depth, nd: no data, SCM: subsurface chlorophyll maximum, Xeq: gum xanthan equivalent

	Layer	TEP (µg Xeq l^{-1})	Chl *a* (µg l^{-1})
Nutrient-limited oligotrophic areas			
Western tropical North Pacific	Mixed layer	43.3 ± 7.4[a]	0.053 ± 0.012[a]
	SCM	42.2 ± 9.8[a]	0.258 ± 0.037[a]
Eastern tropical North Pacific (near Hawaii)	Mixed layer	22.5 ± 25.9[b]	0.38–0.63[b]
	Below the MLD	9.2 ± 7.3[b]	nd
Eastern Mediterranean Sea (Levantine Basin)	Mixed layer	116–420[c]	0.04–0.07[c]
	SCM	48–189[c]	~0.32[c]
	300 or 1000 m	83–386[c]	nd
Gulf of Aqaba	Mixed layer	130–222[d]	0.35–1.3[d]
	SCM	106–228[d]	nd
	300 m	23–209[d]	nd
Mediterranean Sea	Mixed layer	19.4–53.1[e]	<0.01[e]
	SCM	9.1–94.3[e]	0.015–1.78[e]
	Below the SCM	4.5–23.5[e]	nd
Eutrophic open oceans			
Eastern temperate-subarctic North Atlantic	Mixed layer	20–60[f]	0.07–0.59[f]
Eastern subarctic North Pacific	Mixed layer	28.7 ± 25.2[b]	0.30–1.72[b]
	Below the MLD	11.6 ± 8.1[b]	nd
Western subarctic North Pacific			
Outside a bloom	Mixed layer	40–60[g]	1–1.9[g]
Inside a bloom	Mixed layer	80–190[g]	4–19.2[g]

[a]This study, [b]Wurl et al. (2011), [c]Bar-Zeev et al. (2011), [d]Bar-Zeev et al. (2009), [e]Ortega-Retuerta et al. (2010), [f]Engel (2004), [g]Ramaiah et al. (2005)

sentative values for the oligotrophic western North Pacific.

The TEP concentration in the surface mixed layer of the investigated area (43.3 ± 7.4 µg Xeq l^{-1}; Table 1) was in the same order of magnitude as those reported in the surface of both oligotrophic ocean and also eutrophic ocean areas, except for the eastern Mediterranean Sea (Bar-Zeev et al. 2011), the Gulf of Aqaba (Bar-Zeev et al. 2009) and the western subarctic North Pacific during phytoplankton blooms (Ramaiah et al. 2005) (Table 2). The TEP concentration in the eastern Mediterranean Sea (Bar-Zeev et al. 2011) and in the Gulf of Aqaba (Bar-Zeev et al. 2009) were higher than the present study, but their samples were collected near the coast and thus TEP concentration is likely to be affected by terrestrial influences. TEP concentration is higher in oligotrophic coastal areas than in oligotrophic oceanic areas (Bar-Zeev et al. 2011, Wurl et al. 2011).

Although TEP concentrations were relatively stable and varied only by 1 order (20–420 µg Xeq l^{-1}) in the oceans shown in Table 2, chl *a* concentrations differed by up to 3 orders (<0.01–19.2 µg l^{-1}) among reported levels (Table 2). When compared with concentrations in the surface water of the western subarctic North Pacific outside of the bloom area (Ramaiah et al. 2005), the TEP concentration in the present study was almost the same level, but the chl *a* concentration was 2 orders lower than in the western subarctic North Pacific outside of the bloom area (Table 2). The ranges of TEP (40–60 µg Xeq l^{-1}) and chl *a* concentrations (1–1.9 µg l^{-1}) in the surface of the western subarctic North Pacific (Table 2) indicate that the TEP:chl *a* concentration ratio must be in the range of 20–60 in this area, but the exact ratio could not be calculated from the values in Ramaiah et al. (2005). Thus, the TEP:chl *a* ratio in the surface water of the present study (Table 1) is approximately 20 times higher than in the western subarctic North Pacific. The data sets of TEP and chl *a* concentrations from other papers (Table 2) support that the TEP:chl *a* concentration ratio widely varies for oceans. For example, even though the exact ratio also could not be calculated, the ratios are presumed to be $>10^3$ in the eastern Mediterranean Sea when looking at the ranges of TEP and chl *a* concentration in Bar-Zeev et al. (2011). These widely varying TEP:chl *a* concentration ratios imply that TEP concentration, although associated with phytoplankton abundance (Passow 2002b), is also a factor of various, as yet undetermined, biological and physical processes. The relatively high TEP:chl *a* concentration ratio in our study area was possibly due to the strong nitrogen limitation (Fig. 2e) and strong irradiation which promote TEP production by phytoplankton (Passow 2002b). Furthermore, the active regeneration process in an oligotrophic ocean (Capblancq 1990) possibly increases TEP concentration, because bacteria and other heterotrophic organisms also produce TEP and/or its precursors (Passow 2002a, Sugimoto et al. 2007).

TEP concentrations in the subsurface layers (Table 2) were the same level as in the Mediterranean Sea (Ortega-Retuerta et al. 2010, Bar-Zeev et al. 2011), but 2 times higher than in the other ocean areas (Wurl et al. 2011). In the subsurface layers, chl *a* concentrations were higher than in other eutrophic oceans because of the existence of SCM. Therefore, in this area, biotic TEP production was suggested to be high and the TEP concentration of the subsurface layers was elevated.

Subsurface maximum and minimum TEP concentration

Our results of the vertical profile of mean TEP concentration in the oligotrophic western North Pacific, which had a subsurface maximum in the OSS layer (70 ± 21 m) and minimum in the negative $PreNO_3$ layer (188 ± 16 m; Figs. 3 & 4, Table 1), was similar to that reported in other oligotrophic ocean areas (Ortega-Retuerta et al. 2010, Bar-Zeev et al. 2011, Wurl et al. 2011). The subsurface maximum of the TEP concentration in the layer from the bottom of the mixed layer to the SCM was the same characteristic as in the vicinity of Hawaii Island (Wurl et al. 2011), and the subsurface minimum around the SCM or deeper layer was observed in the Mediterranean Sea (Ortega-Retuerta et al. 2010, Bar-Zeev et al. 2011). These reported observations were not investigated at a sufficiently high resolution in the subsurface layers (only 1 or 2 depths) to allow description of the layers, and subsequently we are not able to describe details of the vertical profiles. Our high-resolution observations in the subsurface layer of the oligotrophic ocean area were able to indicate that the TEP concentration had both a subsurface maximum and minimum. Interestingly, the swimming depth of Japanese eel larvae during nighttime (50–125 m; Otake et al. 1998) showed close agreement with the depth of the TEP subsurface maximum (the OSS layer; 70 ± 16 m).

The vertical variation of TEP concentration was not associated with chl *a* concentration, and thus standing stock phytoplankton abundance was not a controlling factor of the TEP concentration in our study area. In the TEP subsurface maximum layer, the DO

concentration was supersaturated (Figs. 2 & 4). DO concentration is an indicator of the net community production in strongly stratified oligotrophic oceans (Riser & Johnson 2008). Therefore, the subsurface maximum of the TEP concentration was suggested to be created by active biotic TEP production based on photosynthesis. However, the lower DO concentration in the surface mixed layer than in the subsurface layer is mainly due to oxygen emissions to the atmosphere, and thus TEP concentration should not decrease in the surface mixed layer if TEPs are only produced by active photosynthesis. Although the factors controlling TEP concentration remain unclear in the present study, possible factors for the low TEP concentration in the surface mixed layer include that TEP can be transported by bubble adsorption to the surface and trapped in the surface microlayer (Zhou et al. 1998, Azetsu-Scott & Passow 2004, Wurl et al. 2011), and can be decomposed by photolysis (Ortega-Retuerta et al. 2009) and also consumed by heterotrophic organisms (Passow 2002b).

The lowest TEP concentration was obtained from the negative $PreNO_3$ layer in the present study, but it had a large variability (Fig. 4). In the deeper layer, the TEP concentration increases by abiotic TEP production (Bar-Zeev et al. 2011). The high variability of the TEP concentration in the subsurface layers may be due to whether marine snow occurs in the sampled water or not, because Brunt–Väisälä frequencies were high in these layers (Table 1, Fig. 2b), where marine snow, which contains a large amount of TEPs, can easily be trapped (MacIntyre et al. 1995). The high Brunt–Väisälä frequencies indicate that minimal water turbulence occurs, which is important for the formation of abiotic TEP coagulation as well as Brownian motion and laminar shear (Burd & Jackson 2009). The negative $PreNO_3$ water is formed by preferential decomposition of carbon-rich and nitrogen-poor DOM (Emerson & Hayward 1995, Abell et al. 2005), which is the precursor of TEPs (Passow 2000, 2002b). Thus, the low abiotic TEP production possibly formed the TEP subsurface minimum in the negative $PreNO_3$ layer because of the low water turbulence and the low amount of precursors of TEP, though the contribution of heterotrophic organisms remains unknown.

CONCLUSION

In the present study, the concentration and vertical profile of TEP was, for the first time, obtained from the oligotrophic western tropical North Pacific. Its concentration was approximately the same as the concentrations in other open ocean areas regardless of phytoplankton abundance or nutrient concentrations. In addition, based on our high-resolution observations in the subsurface layers, it was clarified that vertical profiles of TEP concentration have a subsurface maximum in the OSS layer and minimum in the negative $PreNO_3$ waters. The TEP amount and vertical profile of TEP concentration did not show a clear correlation with chl *a* concentration. Therefore, phytoplankton abundance is not considered to be an index of TEP concentration in the oligotrophic western tropical North Pacific; however, further clarification of the mechanism of TEP production in oligotrophic waters is clearly needed.

Acknowledgements. We thank Captain Y. Terada, officers, crew members and scientists, especially Prof. J. Aoyama and Drs. S. Ijiri, N. Mochioka and S. Watanabe, on the R/V 'Kaiyo-maru' cruise for their cooperation at sea. Oceanic data during the survey were also provided by the R/V 'Natsushima', JAMSTEC (Japan Agency for Marine-Earth Science and Technology). We thank 3 anonymous reviewers for their valuable comments and suggestions to improve the quality of the paper, and Japan Scientific Text for the English language review. This study was financially supported by subsidies from the Fisheries Agency and Fisheries Research Agency.

LITERATURE CITED

Abell J, Emerson S, Keil RG (2005) Using preformed nitrate to infer decadal changes in DOM remineralization in the subtropical North Pacific. Global Biogeochem Cycles 19: GB1008, doi:10.1029/2004GB002285

Alldredge AL, Passow U, Logan BE (1993) The abundance and significance of a class of large, transparent organic particles in the ocean. Deep-Sea Res I 40:1131–1140

Azetsu-Scott K, Passow U (2004) Ascending marine particles: significance of transparent exopolymer particles (TEP) in the upper ocean. Limnol Oceanogr 49:741–748

Bar-Zeev E, Berman-Frank I, Stambler N, Dominguez EV and others (2009) Transparent exopolymer particles (TEP) link phytoplankton and bacterial production in the Gulf of Aqaba. Aquat Microb Ecol 56:217–225

Bar-Zeev E, Berman T, Rahav E, Dishon G, Herut B, Kress N, Berman-Frank I (2011) Transparent exopolymer particle (TEP) dynamics in the eastern Mediterranean Sea. Mar Ecol Prog Ser 431:107–118

Burd AB, Jackson GA (2009) Particle aggregation. Annu Rev Mar Sci 1:65–90

Capblancq J (1990) Nutrient dynamics and pelagic food web interactions in oligotrophic and eutrophic environments: an overview. Hydrobiologia 207:1–14

Chow S, Kurogi H, Mochioka N, Kaji S, Okazaki M, Tsukamoto K (2009) Discovery of mature freshwater eels in the open ocean. Fish Sci 75:257–259

Emerson S, Hayward TL (1995) Chemical tracers of biological processes in shallow waters of North Pacific: preformed nitrate distributions. J Mar Res 53:499–513

Engel A (2004) Distribution of transparent exopolymer particles (TEP) in the Northeast Atlantic Ocean and their potential significance for aggregation processes. Deep-Sea Res I 51:83–92

Hydes D, Aoyama M, Aminot A, Bakker K and others (2010) Determination of dissolved nutrients (N, P, Si) in seawater with high precision and inter-comparability using gas-segmented continuous flow analysers. In: The GO-SHIP repeat hydrography manual: a collection of expert reports and guidelines, Vol 14. IOCCP (International Ocean Carbon Coordination Project), p 87. Available at: www.go-ship.org/HydroMan.html

Johnson KS, Riser SC, Karl DM (2010) Nitrate supply from deep to near-surface waters of the North Pacific subtropical gyre. Nature 465:1062–1065

Kurogi H, Okazaki M, Mochioka N, Jinbo T and others (2011) First capture of post-spawning female of the Japanese eel *Anguilla japonica* at the southern west Mariana ridge. Fish Sci 77:199–205

Levitus S (1982) Climatological atlas of the world ocean. NOAA Prof Paper No. 13, US Government Printing Office, Washington, DC, p 173

Longhurst AR (2006) Ecological geography of the sea. Academic Press, New York, NY

MacIntyre S, Alldredge AL, Gotschalk CC (1995) Accumulation of marine snow at density discontinuities in the water column. Limnol Oceanogr 40:449–468

Miller MJ, Chikaraishi Y, Ogawa NO, Yamada Y, Tsukamoto K, Ohkouchi N (2013) A low trophic position of Japanese eel larvae indicates feeding on marine snow. Biol Lett 9:20120826

Ortega-Retuerta E, Passow U, Duarte CM, Reche I (2009) Effects of ultraviolet B radiation on (not so) transparent exopolymer particles. Biogeosciences 6:3071–3080

Ortega-Retuerta E, Duarte CM, Reche I (2010) Significance of bacterial activity for the distribution and dynamics of transparent exopolymer particles in the Mediterranean Sea. Microb Ecol 59:808–818

Otake T, Inagaki T, Hasumoto H, Mochioka N, Tsukamoto K (1998) Diel vertical distribution of *Anguilla japonica* leptocephali. Ichthyol Res 45:208–211

Passow U (2000) Formation of transparent exopolymer particles, TEP, from dissolved precursor material. Mar Ecol Prog Ser 192:1–11

Passow U (2002a) Production of transparent exopolymer particles (TEP) by phyto- and bacterioplankton. Mar Ecol Prog Ser 236:1–12

Passow U (2002b) Transparent exopolymer particles (TEP) in aquatic environments. Prog Oceanogr 55:287–333

Passow U, Alldredge AL (1994) Abiotic formation of transparent exopolymer particles (TEP) from polysaccharides excreted by phytoplankton. Abstr Pap Am Chem Soc 207:178

Passow U, Alldredge AL (1995) A dye-binding assay for the spectrophotometric measurement of transparent exopolymer particles (TEP). Limnol Oceanogr 40:1326–1335

Passow U, Alldredge AL, Logan BE (1994) The role of particulate carbohydrate exudates in the flocculation of diatom blooms. Deep-Sea Res I 41:335–357

Ramaiah N, Takeda S, Furuya K, Yoshimura T and others (2005) Effect of iron enrichment on the dynamics of transparent exopolymer particles in the western subarctic Pacific. Prog Oceanogr 64:253–261

Riser SC, Johnson KS (2008) Net production of oxygen in the subtropical ocean. Nature 451:323–325

Sugimoto K, Fukuda H, Baki MA, Koike I (2007) Bacterial contributions to formation of transparent exopolymer particles (TEP) and seasonal trends in coastal waters of Sagami Bay, Japan. Aquat Microb Ecol 46:31–41

Suzuki R, Ishimaru T (1990) An improved method for the determination of phytoplankton chlorophyll using N,N-dimethylformamide. J Oceanogr Soc Jpn 46:190–194

Tsukamoto K, Chow S, Otake T, Kurogi H and others (2011) Oceanic spawning ecology of freshwater eels in the western North Pacific. Nat Commun 2:179

Welschmeyer NA (1994) Fluorometric analysis of chlorophyll-*a* in the presence of chlorophyll-*b* and pheopigments. Limnol Oceanogr 39:1985–1992

Wunsch C, Ferrari R (2004) Vertical mixing, energy, and the general circulation of the oceans. Annu Rev Fluid Mech 36:281–314

Wurl O, Miller L, Vagle S (2011) Production and fate of transparent exopolymer particles in the ocean. J Geophys Res Oceans 116:C00H13, doi:10.1029/2011JC007342

Zhou J, Mopper K, Passow U (1998) The role of surface-active carbohydrates in the formation of transparent exopolymer particles by bubble adsorption of seawater. Limnol Oceanogr 43:1860–1871

Editorial responsibility: Ronald Kiene, Mobile, Alabama, USA

Submitted: January 15, 2014; Accepted: July 18, 2014
Proofs received from author(s): September 22, 2014